Journal of Power Sources 196 (2011) 4506–4514

Contents lists available at ScienceDirect

Journal of Power Sources

journal homepage: www.elsevier.com/locate/jpowsour

Platinum catalyst degradation in phosphoric acid fuel cells for stationary applications

T.T. Aindow*, A.T. Haug[1], D. Jayne[2]

UTC Power Corporation, 195 Governor's Highway, South Windsor, CT 06074, USA

ARTICLE INFO

Article history:
Received 15 November 2010
Received in revised form 6 January 2011
Accepted 7 January 2011
Available online 19 January 2011

Keywords:
PAFC
Cathode catalyst
Catalyst degradation
Electrochemical surface area
Platinum particle migration
Particle coalescence

ABSTRACT

A study is presented on the degradation of platinum alloy cathode catalysts operated in phosphoric acid fuel cells. The impact of time and temperature on the fundamental decay mechanism was studied with a surface area loss model and experimental electrochemical surface area measurements. It is suggested that platinum particle migration on the carbon support surface is the dominant mechanism for surface area change in these catalysts.

1. Introduction

High surface area platinum supported on carbon is the preferred choice of catalyst material for fuel cells because it provides enhanced activity at lower cost than bulk platinum (i.e. platinum black). Unfortunately, the small particle sizes needed to provide this large surface area also provide a high driving force for particle coarsening; this leads to surface area loss and, in turn, performance loss. Such degradation is, in particular, an issue for phosphoric acid fuel cells (PAFCs), which have inherently lower performance than other technologies like polymer electrolyte membrane (PEM) fuel cells due to the large Tafel slope (>90 mV; [1]) and strong interactions between phosphate ions and platinum. There is a substantial amount of literature concerning platinum surface area loss both from theoretical and from experimental standpoints. In general, two main mechanisms have been identified to be responsible for platinum surface area loss: a dissolution-reprecipitation mechanism and a particle migration-coalescence mechanism [2]. The former is often referred to as 'Ostwald ripening' whereby platinum dissolves and forms ions in the electrolyte and subsequently re-deposits onto larger crystallites. The second mechanism is sometimes referred to as 'particle diffusion' in which platinum crystallites migrate on the support surface and can impinge and merge to form larger particles.

Platinum dissolution in PAFCs has been recognized as a significant issue for long-term performance. Connolly et al. [3] first proposed such a mechanism in 1966 after they observed a higher rate of surface area loss than that which could be accounted for by particle sintering (for instance, in air or argon atmospheres). They suggested that small and large particles can form local cells with the small particles serving as anodes due to their higher surface energy. Subsequently, Bindra et al. [4] studied the equilibrium solubility of platinum in phosphoric acid using gravimetric measurements. These authors found that the solubility of platinum is a function of potential and that holding the cathode potential at above 0.8 V led to significant platinum loss. Honji et al. [5] investigated the rate of platinum surface area loss in phosphoric acid under air and N_2 atmospheres. They found that under N_2 the potential was relatively low (0.3 V) and a minimal loss of surface area was observed. This was in contrast to the result obtained in phosphoric acid under air, for which the potential was higher and the loss of surface area was larger. Aragane et al. [6] observed significant cathode platinum loss as well as platinum precipitation in the SiC matrix, just outside the cathode catalyst layer. They attributed the platinum precipitation to dissolution and proposed that these phenomena occurred as a result of unintentional potential excursions during start-up and shut-down. Interestingly, Aragane et al.'s observations are similar to those observed in PEM fuel cells for transportation applications. In addition to the high potential, Kinoshita et al. [7] showed that cycling also enhances platinum dissolution. This is

* Corresponding author. Tel.: +1 860 727 2312; fax: +1 869 998 8229.
E-mail address: tai-tsui.aindow@utcpower.com (T.T. Aindow).
[1] Now at 3M Corporation, St. Paul, MN 55144, USA.
[2] Now at Evonik Industries, Mapleton, IL 61547, USA.

0378-7753/$ – see front matter © 2011 Elsevier B.V. All rights reserved.
doi:10.1016/j.jpowsour.2011.01.027

because a platinum oxide layer forms at high constant potential, and can protect the platinum from further dissolution (i.e. passivation). However, when the potential is cycled, there will be enhanced dissolution during the potential ramp-up (anodic direction) because the protective oxide layer has not yet formed. Overall, the consensus amongst researchers is that platinum dissolution can be minimized by controlling the cathode potential to values below 700–750 mV.

Other researchers have invoked platinum crystallite migration on the support surface to explain surface area loss. Bett et al. [8] studied the platinum surface area loss in gas and liquid environments. They found that exposure to gas environments did not lead to significant area loss below 600 °C, which is in contrast to the behavior during exposures to liquid environments. They reported that the potential did not have a significant impact on the rate of surface area loss, and that the activation energy in liquids is smaller than that in gases. These authors attributed platinum surface area loss to crystallite migration (i.e. Smoluchowski mechanism). Blurton et al. [9] also reported that the potential had little effect on the rate of platinum surface area loss. They found that the rate of surface area loss instead depends on the nature of the support surface (e.g. metal catalyzed oxidation vs. uncatalyzed oxidation) and concluded that particle migration is responsible for Pt surface area loss in phosphoric acid electrolytes. Stonehart and Zucks [10] also concluded that the loss of Pt surface area was due to particle migration, although they suggested that potential changes can alter the interaction between the support and the metal crystallite giving rise to variations in sintering rate. The most conclusive evidence for the particle migration mechanism is that reported by Gruver et al. [11], who investigated the sintering of platinum supported on carbon in phosphoric acid using TEM. Not only did they observe clustering of platinum particles after exposure in phosphoric acid, but they also found the presence of particles in regions that were blocked off initially during platinum deposition. These authors also concluded that for values below 750 mV, the potential had a minimal impact on the rate of surface area loss. For a more detailed review of the two mechanisms discussed, the reader is directed to Kinoshita's review paper [12].

Irrespective of the exact mechanism involved, the change in surface area can be described by the following mathematical expression:

$$\frac{1}{S^{n-1}} = \frac{1}{S_0^{n-1}} + kt \quad (1)$$

where S_0 and S represent the surface area per unit volume before and after aging for a time t, respectively. Bett et al. [8] suggested that the mechanism could be derived from the values of the constants, k and n, in this equation. For the dissolution-precipitation mechanism, the rate constant, k, does not depend on the platinum loading. This is in contrast to the particle migration-coalescence mechanism whereby k is a function of platinum loading. The migration-coalescence mechanism can be considered as a two-step process; particle migration on the support surface followed by coalescence after particle impingement. Ruckenstein and Pulvermacher [13,14] tried to further differentiate which of these two steps is rate-limiting. These authors used a mathematical treatment corresponding to two-dimensional Brownian motion and concluded that the exponent, n, derived from fitting experimental data to Eq. (1) can be used to determine the rate-controlling step. They suggested that for n smaller than 3, surface area loss is dominated by the coalescence step whereas for n greater than 3, particle migration is the rate-limiting step.

In this paper, a study of the impact of time and temperature on the degradation for platinum alloy PAFC catalysts is presented.

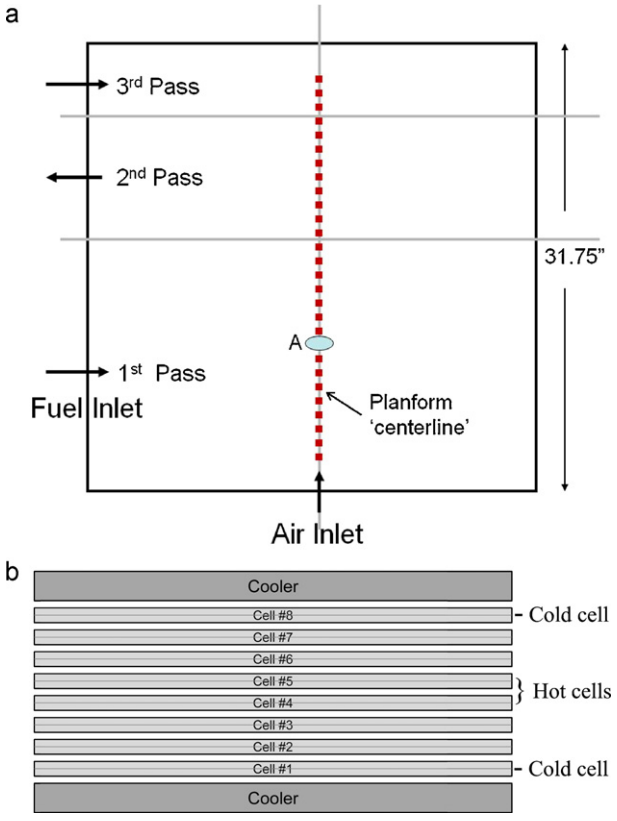

Fig. 1. Schematic diagrams showing: (a) the cell plan-form; electrode samples were extracted along the centerline parallel to the airflow direction as shown by the red squares; (b) the configuration of a 'substack'. (For interpretation of the references to color in this figure legend, the reader is referred to the web version of the article.)

The catalysts were studied both for different locations within a cell and for different cells within a stack to assess the effects of temperature as significant thermal gradients exist during steady-state operation. Surface area was investigated using ex situ techniques including electrochemical and microscopic methods. Performance was measured by reconstructing sub-scale cells with aged catalyst layers that had been extracted from the full-sized operated cells. The resulting data were then used to deduce the mechanisms that are responsible for the platinum surface area loss in these fuel cells.

2. Experimental

The plan-form geometry for the type of cells studied here is illustrated in Fig. 1(a); this design has a single-pass air flow and a three-pass fuel flow using external manifolds. Cells are serialized into units of eight, referred to as 'sub-stacks', which are separated by coolers (Fig. 1(b)). There are 32 sub-stacks in a stack. Within each sub-stack, the cells adjacent to the coolers experience lower temperatures during operation than those cells in the center of the sub-stack. Cells No. 1 and No. 8 are, therefore, referred to as 'cold' cells whereas cells No. 4 and No. 5 are 'hot' cells. In this study, analyses were performed on hot and cold cells after 5000, 9000, 32,000, 43,000, 44,000 and 50,000 h of operation under similar conditions.

The chosen cells were sectioned across the centerline in the direction of cathode air flow and electrode samples of 1 cm^2 area were extracted along this section. The electrochemical surface areas of the catalyst layers were measured using linear potentiodynamic sweeps (or cyclic voltammetry). These measurements were performed in a three-chamber cell on flooded catalyst layers at room temperature. The potential sweeps were taken from

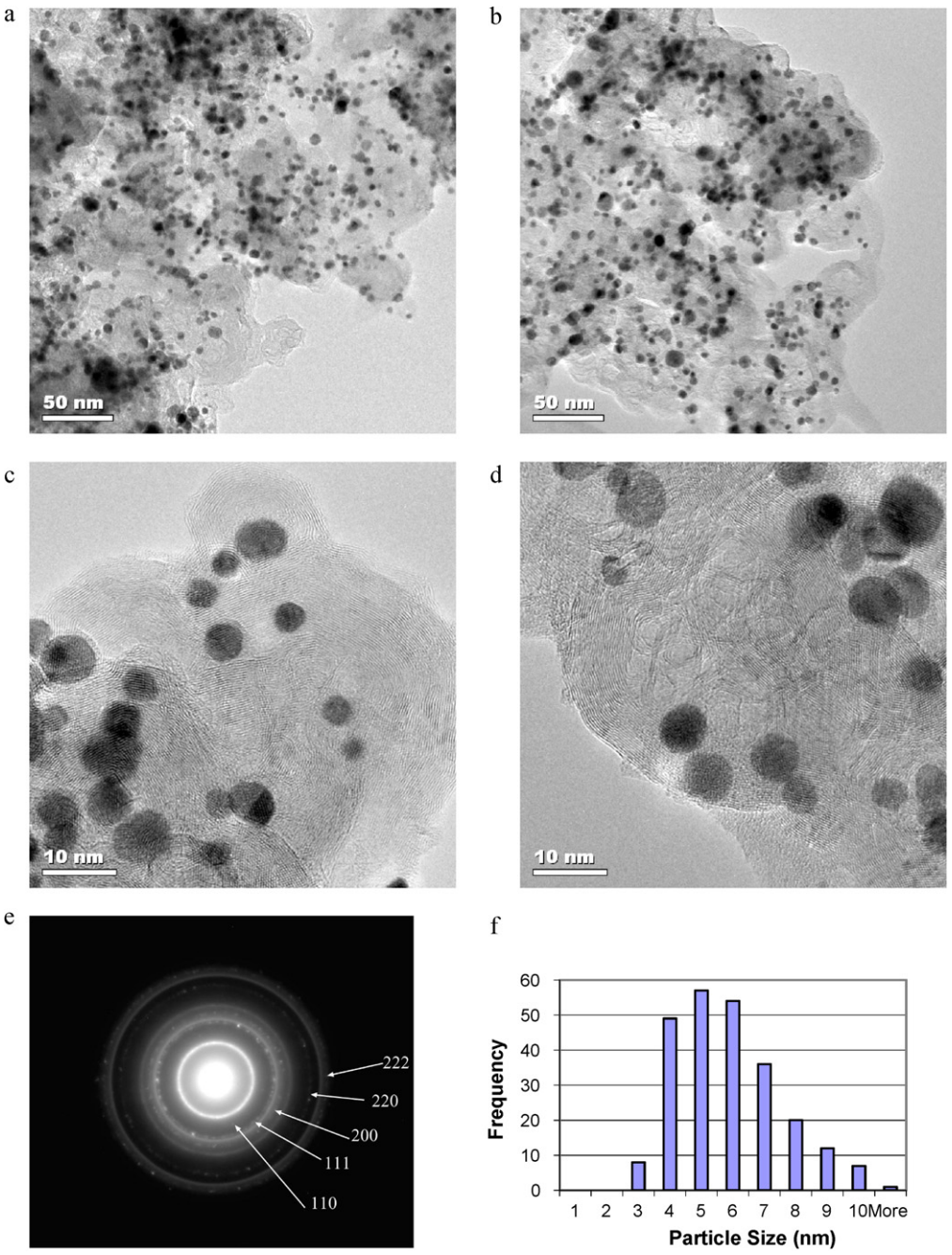

Fig. 2. (a)–(d) TEM images obtained from baseline/virgin cathode catalyst layer, (e) selected area diffraction pattern, and (f) histogram of Pt particle size distribution.

0.01 V to 1.2 V at a rate of 33 mV s^{-1} using Pt/H_2 as a reference in 1 M H_3PO_4. The platinum crystallite size distributions were determined from transmission electron microscopy (TEM) images obtained using a JEOL 2010 FasTEM microscope operated at 200 kV. Macroscopically, the metal loading (platinum and alloying elements) per electrode unit area were analyzed using ICP after digesting the electrode in *aqua regia* solution. Although both anode and cathode electrodes have been investigated in the current study, only degradation in the cathode is discussed in the current paper. The cathodes analyzed have a catalyst consisting of 15 wt%-$Pt_{0.58}Co_{0.24}Cr_{0.18}$ supported on *graphitized* Vulcan XC-72. This cathode catalyst was developed at UTC Power by Luczak and Landsman [15] specifically for the PC25^{TM} series fuel cells used in this study. The catalysts were bonded with Teflon to form porous electrodes in the fuel cells. The nominal platinum loading per unit electrode area is 0.75 mg cm^{-2}.

To assess the impact of catalyst degradation on performance, samples were extracted from aged cathodes and were built into single-cell assemblies using new anodes and gas diffusion layers. This procedure allows us to isolate the impact of cathode catalyst on performance. Performance over a range of temperatures, acid concentrations, CO concentrations and oxygen partial pressures were measured. The current work focuses on subscale results obtained under H_2–Air and H_2–O_2 operating conditions. In order to examine decay over a large range of temperatures and operating conditions, samples were extracted from several areas within the planform, including the hottest active areas from hot cells and the coldest active areas from cold cells.

3. Results

3.1. Baseline virgin catalyst

As noted in the preceding section, the cathode catalyst used in these PAFCs was a 15 wt%-$Pt_{0.58}Co_{0.24}Cr_{0.18}$ catalyst supported on *graphitized* Vulcan XC-72. Potentio-dynamic (or cyclic voltammetry) sweeps obtained from a pristine catalyst showed that the catalyst had an initial electrochemical area (ECA) of ~50 $m^2\ g_{Pt}^{-1}$. The platinum crystallite size and distribution were characterized using TEM. Fig. 2(a)–(d) shows the TEM images obtained from the pristine catalyst. The particle sizes were measured from a series of such images and the cumulative particle size distributions were analyzed. Fig. 2(f) is a histogram showing the particle size distribution for a sample size of ~250 particles. It is noted that the particles are between 3 and 10 nm in diameter with an average diameter of 5.3 nm. This value corresponds to a Pt surface area of ~52 $m^2\ g^{-1}$ assuming a mono-disperse particle size distribution which is in good agreement with the ECA measurement. Electron diffraction was used to identify lattice ordering in the crystal structure of the platinum alloy. Fig. 2(e) is an example of a selected area diffraction pattern showing the presence of super-lattice diffraction maxima (e.g. the 110 spot) in addition to the usual rings from f.c.c. Pt. Such spots demonstrate that there is superlattice ordering of the crystal structure. We note that Luczak and Landsman [15] suggested that lattice ordering can enhance oxidation reduction activity of platinum alloy catalysts.

3.2. Aged catalysts from hot cells

Cells were removed from stacks that had varying durations of operation. As discussed in Section 2, depending on the distance from the cooler in a sub-stack, the cells had different operating temperatures and are categorized as hot or cold cells. The platinum alloy catalyst decay was characterized by extracting about thirty 1 cm^2 samples from different regions of each cell. Fig. 1(a) shows the locations of the samples with respect to the cell plan-form. These are along the air-inlet to air-exit orientation, which is referred to as the 'centerline'. ECA measurements were performed on these extracted samples. The results from hot cells are discussed in this section. Fig. 3(a) shows the ECA results obtained from a hot cell in a stack that had ~9000 h of operation. The ECA at the air inlet region is ~18 $m^2\ g^{-1}$, and decreases to ~14 $m^2\ g^{-1}$ at a distance of 10 in. from the air inlet. The highest ECA value is obtained at the air exit (~28 $m^2\ g^{-1}$). It is noted that centerline ECA data were obtained on all of the stacks investigated but only selected data sets are presented in this paper for brevity. Fig. 3(b) shows another set of centerline ECA measurements which were extracted from a hot cell that had ~43,000 h of operation. Here again, the ECA decreases from the air inlet (~14 $m^2\ g^{-1}$) and the minimum value is obtained at ~10 in. from the air inlet (~6 $m^2\ g^{-1}$).

The Pt alloy crystallite sizes in these samples were studied using TEM. Fig. 4(a)–(d) shows the TEM images obtained from the 9000 h hot cell at location 'A' as indicated in Fig. 1(a). It is evident that the crystallites in this sample are larger than those observed in the pristine sample and range between 5 and >50 nm in diameter. The diffraction patterns obtained from these samples (e.g. Fig. 4(e)) show that the crystal structure remains ordered. The metal loading

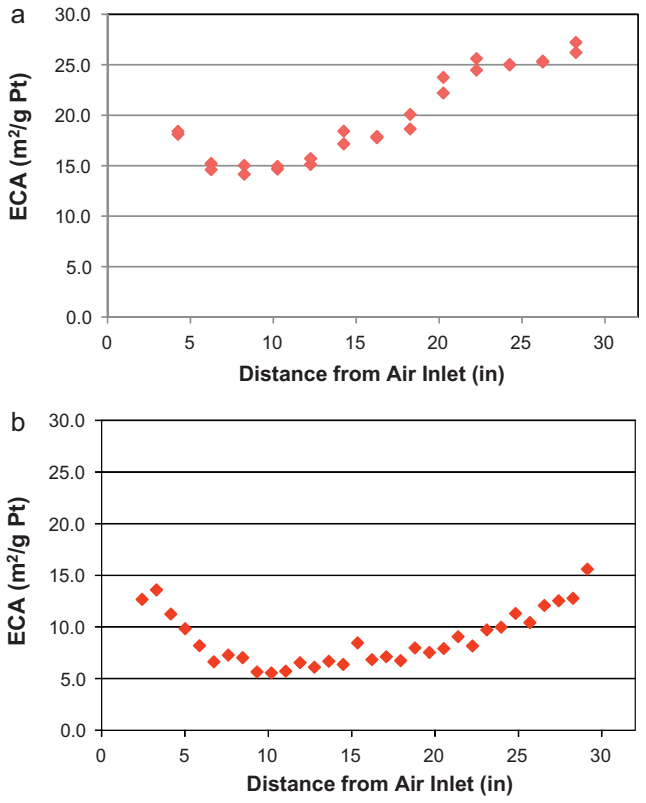

Fig. 3. (a) ECA measurements obtained from the centerline of a hot cell after 9000 h, (b) Centerline ECA data obtained from a hot cell after 43,000 h.

in the sample was analyzed using ICP and the results are shown in Table 1. These data suggest that the catalyst suffered minimal loss of platinum, whereas there was significant loss of the alloying elements Co and Cr. This is reflected in the higher atomic percent of platinum.

Samples of a hot cell with 43,000 h of operation were also investigated using TEM, and examples of the images are presented in Fig. 5(a)–(d). It can be seen that the particle population is significantly reduced compared with the pristine sample. The particle size distribution (Fig. 5(f)) shows that the average size of ~20 nm is nearly four times higher than that of the pristine catalyst. We note that the ECA measured, ~6 $m^2\ g^{-1}$, is significantly less than the value of ~14 $m^2\ g^{-1}$ expected based on the average particle size. This suggests that the particle size distribution in the sample is no longer mono-disperse. ICP analyses obtained from this catalyst are also shown in Table 1. Here again, the results suggest that the platinum loss in the catalyst was insignificant whereas the majority of the Co and Cr had leached out. This is confirmed by the analyses of the H_3PO_4 electrolyte present in the cell; these data show significant concentrations of Co and Cr, whereas no platinum has been detected. Electron microprobe analysis (EMPA) was used to map the platinum in these samples to study the possibility of Pt precipitation in the matrix as observed by Aragane et al. [6]. Examples of these maps obtained from hot and cold cells are presented in Fig. 6(a) and (b). No significant Pt precipitation in the matrix is observed.

Table 1
ICP results obtained from new and used electrodes.

Operation (h)	Average particle size (nm)	ECA ($m^2\ g^{-1}$)	Pt loading (mg cm^{-2})	Co loading (mg cm^{-2})	Cr loading (mg cm^{-2})	Composition
0	5.3	50	0.75 ± 0.08	0.095 ± 0.002	0.062 ± 0.001	$Pt_{0.58}Co_{0.24}Cr_{0.18}$
9000	14.8	~14	0.79 ± 0.04	0.031 ± 0.002	0.016 ± 0.001	$Pt_{0.83}Co_{0.11}Cr_{0.06}$
43,000	20.4	~6	0.75 ± 0.02	0.021 ± 0.002	0.009 ± 0.001	$Pt_{0.89}Co_{0.08}Cr_{0.03}$

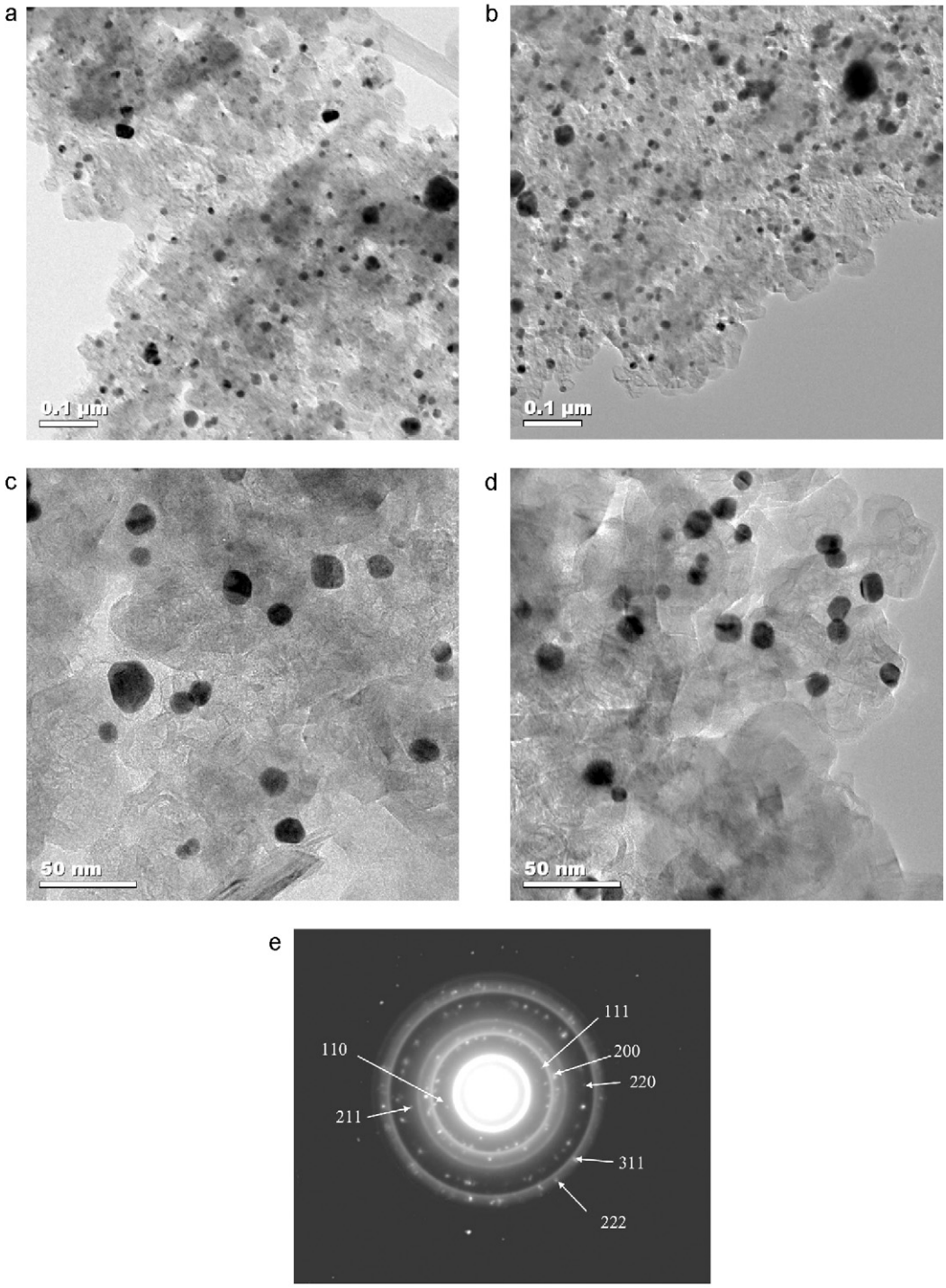

Fig. 4. (a)–(d) TEM images obtained from a hot cell cathode electrode after 9000 h, (e) selected area diffraction pattern.

3.3. Aged catalysts from cold cells

Catalyst degradation was also investigated in cold cells from the same stacks. Here again, ~30 samples were extracted along the centerline in each of the selected cells and ECA measurements were performed using cyclic voltammetry. Fig. 7(a) and (b) shows ECA data from stacks that had 9000 and 43,000 h of operation, respectively. It can be seen that the ECA is 17–26 $m^2\ g^{-1}$ after 9000 h and 8–18 $m^2\ g^{-1}$ after 43,000 h of operation. These values are higher than those obtained from the respective hot cells (see Fig. 3(a) and (b)) although the overall characteristics are similar in that the minima are at a distance of ~10 in. from the air inlet and the maxima are at the air exit.

3.4. Effect of time

Since, as indicated in Eq. (1), surface area is a function of time, it is important to assess the impact of time on catalyst degradation in the cells that are under investigation. As discussed earlier, all of the stacks selected for the current work had similar operating

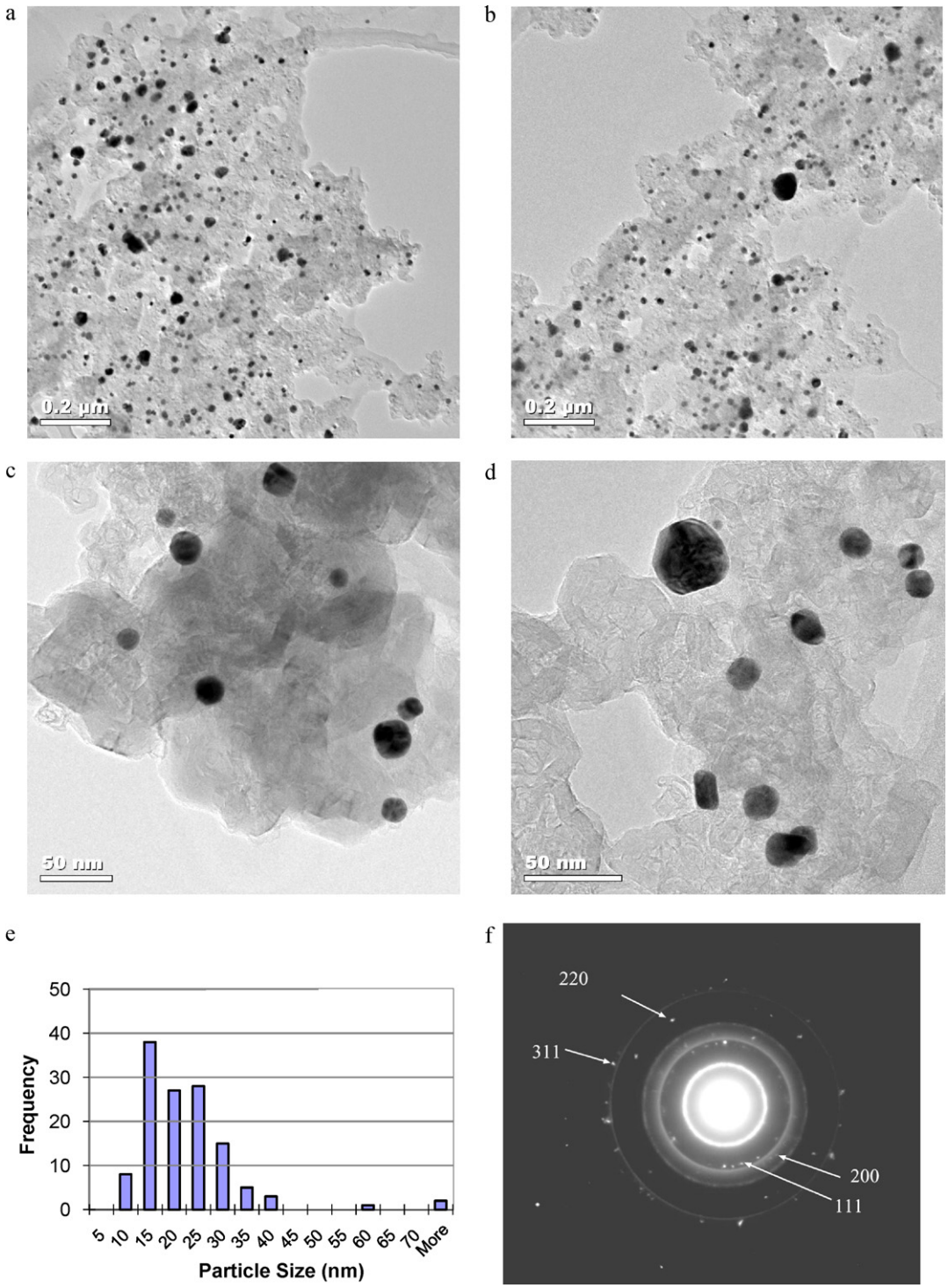

Fig. 5. (a)–(d) TEM images showing hot cell cathode catalyst after 43,000 h, (e) Pt particle size distribution and (f) selected area diffraction pattern.

conditions. Thus, by comparing data obtained from the platinum catalysts in stacks with different durations of operation, but from the same geometric location and cell position in the sub-stack, the impact of operating time can be evaluated. Fig. 8 is a plot of the ECA values obtained from the centerline at ~10 in. from the air-inlet location (i.e. position 'A' indicated in Fig. 1(a)) against operating time for hot and cold cells in each of the sub-stacks studied. At each time the values of ECA for the hot cells are lower than those for the cold cells.

3.5. Impact of degradation on performance

To assess the impact of catalyst degradation on performance, samples were extracted from aged cathodes and were built into 5 cm × 5 cm single-cells. These sub-scale cells were subjected to performance testing and the results were compared with cells constructed using baseline-virgin electrodes. Polarization curves obtained using new electrodes and electrodes taken from the hot cells of stacks operated for 9000 and 43,000 h are shown in Fig. 9.

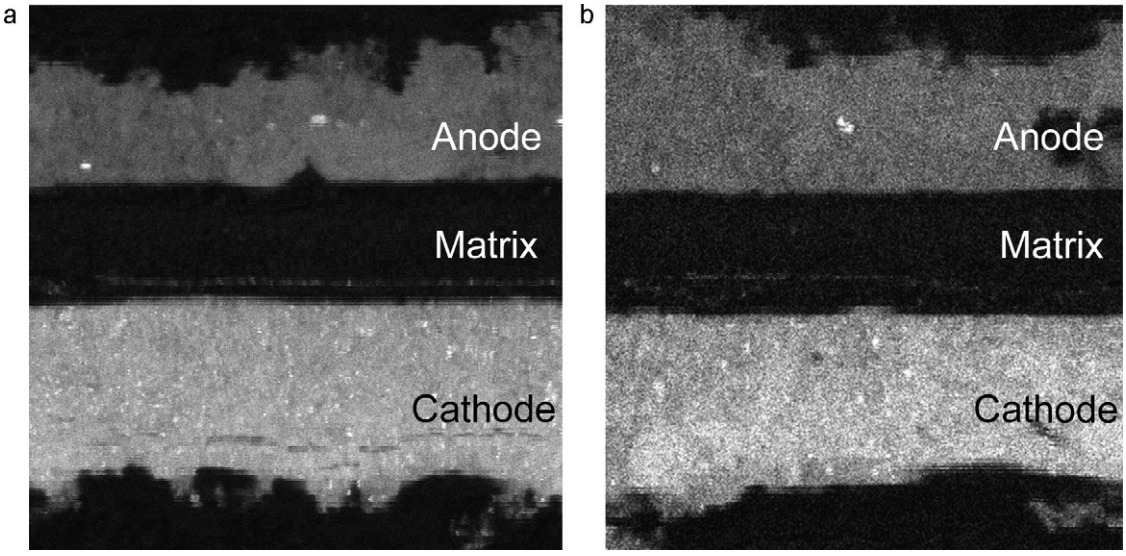

Fig. 6. (a) and (b) EPMA maps obtained from respective hot and cold cell after 43,000 h showing Pt distribution.

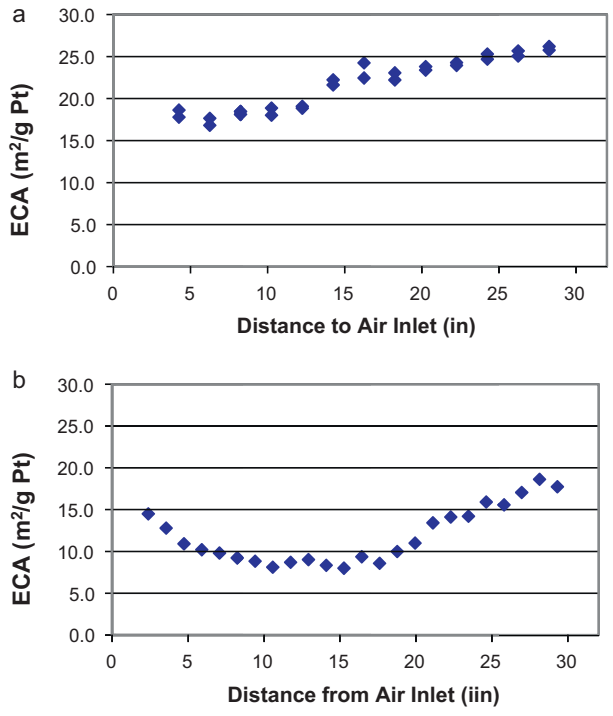

Fig. 7. (a) Centerline ECA data obtained from a cold cell after 9000 h, (b) Centerline ECA data obtained from cold cell after 43,000 h.

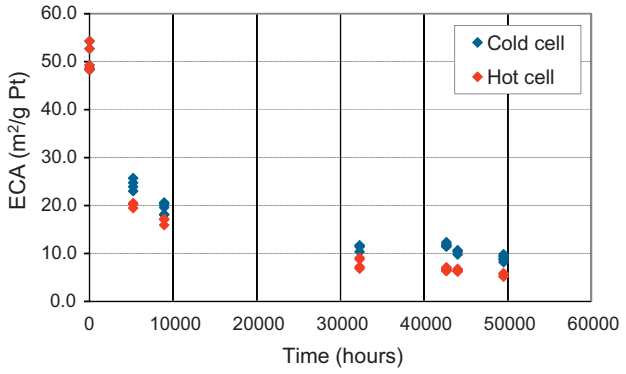

Fig. 8. ECA measurements on hot and cold cells (at location 'A') as a function of time.

At 175 °C, 99% H_3PO_4 and H_2/Air testing conditions, performance decays for the hot cell hot spot, i.e. location 'A', are estimated at 53 mV and 95 mV at 100 mA cm^{-2} after 9000 and 43,000 h, respectively. Based on the slopes of the polarization curves, it is concluded that the resistance difference between new and used electrodes is not significant.

3.6. Numerical modeling of ECA decay

Comparing the ECA data obtained from the hot and cold cells within a particular stack (e.g. the 9000 h or 43,000 h stacks), it is evident that surface area loss is affected mostly by temperature. As would be expected, higher temperature leads to greater surface area loss. The impact of temperature on catalyst decay is also manifested within each cell. Fig. 10 shows the temperature profiles in the hot and cold cells. These cell temperature profiles were obtained by numerical cell/stack modeling using physics-based principles. The model was calibrated using temperature measurements performed in the laboratory. As discussed in Section 1, changes in surface area can be described mathematically by Eq. (1), in which k can be described by the following expression:

$$k = k_0 e^{-E_a/RT} \quad (2)$$

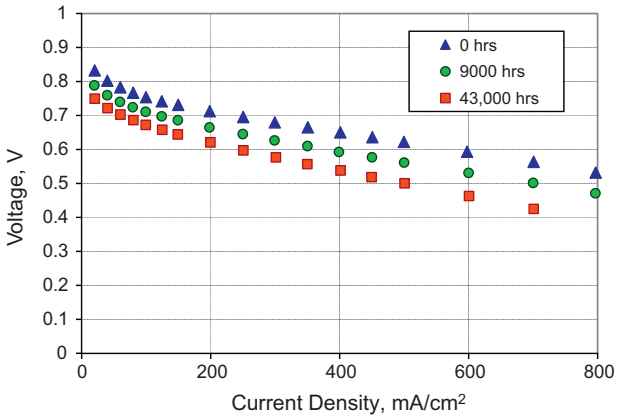

Fig. 9. Polarization curves and IR measurements obtained from new and used (9000 h and 43,000 h) electrodes. Test condition used: 175 °C, 99% H_3PO_4, H_2/Air, 0 psig, stoichiometry (H_2/Air) 3.4/4.0.

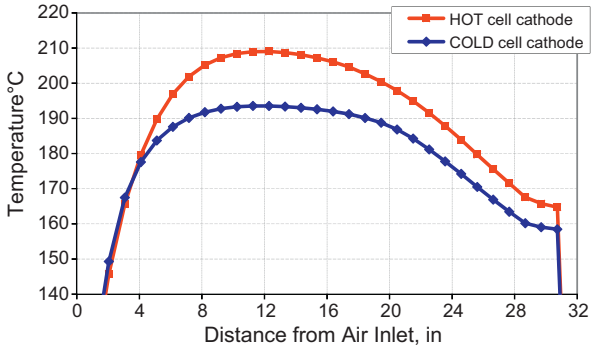

Fig. 10. Centerline temperature profiles in hot and cold cells.

where E_a is the activation energy, and k_0 is the temperature independent rate constant. Fitting Eqs. (1) and (2) to the experimental ECA values obtained from cells with a range of operational lifetime between 0 and 57,000 h shows a reaction order of $n = 3.2$, a k_0 value of 2.98×10^4, and an activation energy $E_a = 180\ \text{kJ mol}^{-1}$. We note that this latter value is somewhat higher than the $85\ \text{kJ mol}^{-1}$ reported by Bett et al. [17] for a PAFC environment, but the origin of this difference is not clear. Fig. 11(a) shows the temperature profile of the hot cell and the ECA data obtained from the stack operated for 43,000 h compared with the predictions of the numerical model. In addition, Fig. 11(b) shows a comparison between experimentally measured ECA values and values from the numerical model for Location 'A' in all the hot and cold cells studied. It can be seen that the correlation between temperature and ECA decay at various locations is remarkable.

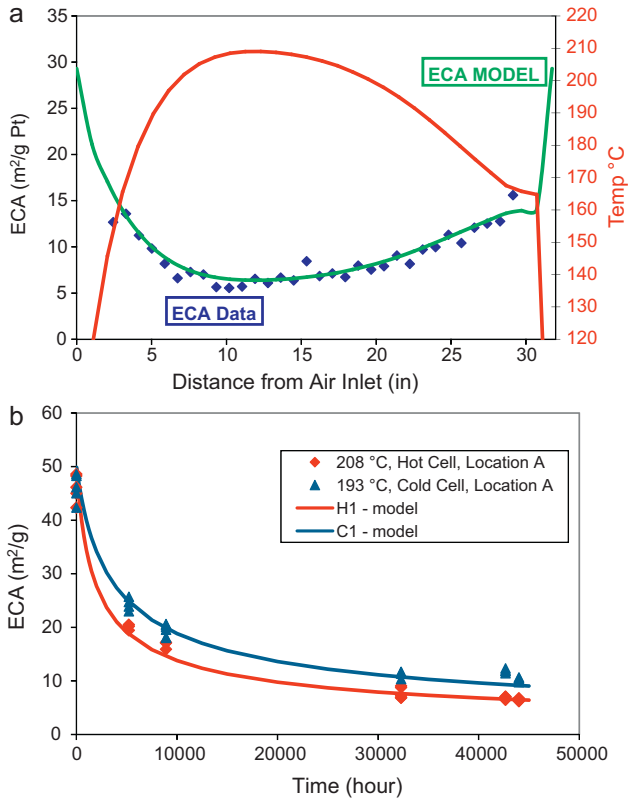

Fig. 11. (a) Centerline temperature vs. ECA observed; (b) Comparison of ECA measurements obtained experimentally and fitted model projection.

4. Discussion

As discussed in Section 1, platinum surface area loss has been attributed to two different mechanisms; dissolution-precipitation and particle migration-coalescence. Granqvist and Buhrman [16] argued that for the particle migration (or Smoluchowski) mechanism there is a cut-off at smaller particle sizes (particles cannot become smaller) and a tail at larger diameters. This is in contrast to the dissolution-precipitation mechanism where large particles grow at the expense of smaller particles so there should always be particles with small sizes. In the current work, no particles with diameters smaller than 5 nm have been observed in samples with 43,000 h of operation. This would suggest that the dissolution-precipitation mechanism is unlikely to be responsible for the observed change in surface area. In addition, no significant loss of platinum has been observed in these samples and this is further supported by the fact that there is no significant precipitation of platinum in the matrix such as that observed by Aragane et al. [6]. This suggests that dissolution is not a main contributor to catalyst degradation. Furthermore, as concluded by many researchers, a pre-requisite for dissolution is high potential. We note that high potentials had been observed in some earlier generations of phosphoric acid power plants when potential excursions such as the ones described by Honji et al. [5] were not mitigated adequately. However, the current generation of power plants typically operates at under 0.7 V and the potentials during start-ups and shut-downs are controlled closely through clip voltage/dummy load. Darling and Meyers [18] concluded that at under 0.7 V the solubility of platinum in phosphoric acid is extremely low. The catalyst surface area loss observed in this study is thus attributed to crystallite migration and coalescence.

For the migration-coalescence mechanism, Ruckenstein and Pulvermacher [13,14] suggested that by obtaining a value for the exponent n in Eq. (1) from the surface area loss data, it can be inferred whether the migration step or the subsequent coalescence step is rate-limiting. For an n value that is greater than 3, migration is rate-controlling whereas for n smaller than 3, coalescence is the rate-limiting step. Since n is found to be 3.2 in the current study, we cannot identify clearly the rate-limiting step on this basis, as the value for n in Eq. (1) lies at the boundary of the migration and coalescence limiting regimes [13,14]. However, we argue that for the wide range of durations included in the current study, it may be overly simplistic to assume that the rate-controlling step for the surface area loss observed is the same over the entire range of durations. In fact, we postulate that for shorter durations, there is a large particle population and the probability of particles impinging on one another is quite high; thus, coalescence is likely to be rate-limiting. At longer durations, fewer particles remain and the likelihood of particles encountering one another is significantly reduced, therefore particle migration would be the rate-controlling step. There is some evidence to support this hypothesis in the TEM images. For example, Fig. 12(a) and (b) shows the images obtained from an experimental prototype stack that had accumulated 5000 h of operation in the laboratory. Evidence of crystallite clumping observed in Fig. 12(a) would imply that particle migration occurs readily and that the rate-controlling step is thus coalescence. Fig. 12(b) shows the presence of micro-twins in the Pt alloy particles also suggesting coalescence of multiple particles. We should also note that after 43,000 h no clusters have been observed which would imply that the migration step is rate-controlling at this point.

It has been well established that platinum surface area loss can lead to performance decay in fuel cells and that the magnitude of the decay can be estimated using the Tafel equation provided that the specific activity remains

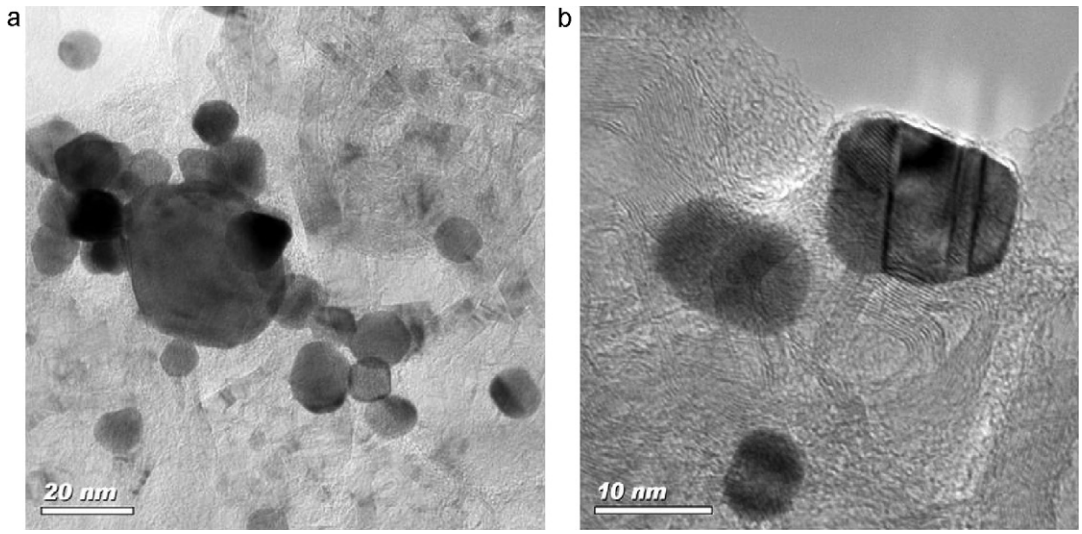

Fig. 12. (a) and (b) TEM images obtained from a 5000 h laboratory-tested prototype stack.

constant:

$$A = B \log\left(\frac{S(t)}{S_0}\right) \quad (3)$$

where A is the voltage decay, B is the Tafel slope, $S(t)$ is the ratio of catalyst surface area at time t, and S_0 is the initial catalyst surface area. The performance decay after 9000 and 43,000 h could thus be estimated based on the changes in ECA values alone as 47 mV and 83 mV, respectively. Because the data were measured at 175 °C and that Tafel slope increases with temperature, a Tafel slope of 90 mV must be used. Performance losses were measured at 100 mA cm^{-2} in H_2/Air using in-cell tests, which show that the performance decay for the hot cell are 53 mV and 95 mV after 9000 and 43,000 h, respectively. These values are larger than the losses estimated using ECA values alone, which is rather surprising since specific activity is expected to increase as the platinum particles become larger [19–21] and thus the performance losses were expected to be less. The larger observed performance losses suggest that other phenomena are contributing to the losses. One probable contributor is that the alloy catalyst had become more pure platinum-like after the majority of the alloying elements, Co and Cr, have leached out. Additionally, the loss of these alloying elements would reduce the degree of lattice ordering which could also lead to decreased activity.

5. Conclusions

A study on the degradation of platinum alloy cathode catalysts in PAFCs has been presented. It has been shown that the rate of change in electrochemical surface area is impacted both by duration and by temperature. Surface area measurements and microscopic data were used to infer the mechanism responsible for the change in surface area. These data are consistent with platinum particle migration on the carbon support surface being the mechanism responsible for the surface area loss in these catalysts.

Acknowledgements

The authors acknowledge Mike Lindsay and Mike Fortin for performing the ECA testing and subscale testing in this work, and Dr. Lichun Zhang at the University of Connecticut for performing the TEM studies. The authors would also like to acknowledge Dr. Mark Aindow, Dr. Ned Cipollini and Dr. Rob Darling for commenting on the manuscript.

References

[1] H.R. Kunz, G.A. Gruver, J. Electrochem. Soc. 122 (1975) 1279–1287.
[2] K. Kinoshita, Electrochem. Oxygen Technol. (1992) 201–205.
[3] J.F. Connolly, R.J. Flannery, B.L. Meyers, J. Electrochem. Soc. 114 (1967) 241–243.
[4] P. Bindra, S.J. Clouser, E. Yeager, J. Electrochem. Soc.: Accelerated Brief Communication September (1979) 1631–1632.
[5] A. Honji, T. Mori, K. Tamura, Y. Hishinuma, J. Electrochem. Soc. 135 (1990) 355–359.
[6] J. Aragane, H. Urushibata, T. Murahashi, J. Appl. Electrochem. 26 (1996) 147–152.
[7] K. Kinoshita, J. Lundquist, P. Stonehart, Electroanal. Chem. Interfacial Electrochem. 48 (1973) 157–166.
[8] J.A. Bett, K. Kinoshita, P. Stonehart, J. Catal. 35 (1974) 307–316.
[9] K.F. Blurton, H.R. Kunz, D.R. Rutt, Electrochim. Acta 23 (1978) 183–190.
[10] P. Stonehart, P.A. Zucks, Electrochim. Acta 17 (1972) 2333–2351.
[11] G. Gruver, R. Pascoe, H. Kunz, J. Electrochem. Soc. 127 (1980) 1219–1224.
[12] K. Kinoshita, ECS (1977) 644–655.
[13] E. Ruckenstein, B. Pulvermacher, J. Catal. 29 (1973) 224–245.
[14] E. Ruckenstein, B. Pulvermacher, AlChE J. 19 (1973) 356–364.
[15] F.J. Luczak, D.A. Landsman, U.S. Patent No. 4,677,092 (1987).
[16] C.G. Granqvist, R.A. Buhrman, J. Catal. 42 (1976) 477–479.
[17] J.A.S. Bett, K. Kinoshita, P. Stonehart, J. Catal. 41 (1976) 124–133.
[18] R.M. Darling, J.P. Meyers, J. Electrochem. Soc. 150 (2003) A1523–A1527.
[19] L. Bregoli, Electrochem. Acta 23 (1978) 489.
[20] M. Watanabe, H. Sei, P. Stonehart, J. Electroanal. Chem. 261 (1989) 375–387.
[21] P.N. Ross, Proc. Electrochem Soc. 175th Meeting Abstract No. 454, 1989.